2006-01-1525

Faster is Better: The Effect of Internal Turbulence on DOC Efficiency

E. Kent Dawson, Ph.D.
Ford Motor Company

Jan Kramer
Emitec, Inc.

ABSTRACT

A number of metallic oxidation catalyst substrates with advanced internal structures have emerged in the past few years. In an aftertreatment application, these structures improve gas mixing by increasing turbulence within the substrate's matrix. Modeling results show these advanced structures, under some operating conditions, can be correlated to reductions in catalyst substrate volume and precious metal [1,2].

Three structured metallics were compared to a baseline ceramic substrate in a designed experiment to understand the effect of advanced metallic substrates on diesel oxidation catalyst (DOC) sizing and performance. The results showed that smaller metallic DOCs coated with up to 30% less precious metal (PM) catalyst performed on par or better than the baseline ceramic DOC in terms of hydrocarbon conversion, heat-up, and pressure drop.

INTRODUCTION

DOCs are used worldwide today for most on-road diesel applications. However, tighter diesel emission standards, starting in North America in 2007, will require DOCs not only to remove hydrocarbons but also to generate significant heat for the regeneration of downstream catalysts and particulate filters.

Under normal conditions the gas flow through conventional continuous monolith channels develops laminar characteristics resulting in a boundary layer. This layer results in restricted mass transfer from the gas to the catalytically coated substrate wall and limits the overall efficiency of the catalyst. In addition, conventional continuous channel catalyst substrates transmit any mixing non-uniformity through the catalyst to any downstream systems.

Previous work has described a number of advanced metallic substrate designs [1,2,3]. These substrates are characterized by partially deformed, interrupted, or laterally offset walls which create flow disturbances and increase mass transfer to the walls. In addition, an interruption of the substrate walls allows flow exchange between the substrate channels, increasing utilization and improving distribution.

TRANSVERSAL FOIL STRUCTURE (TS)

As shown in Figure 1, a TS foil is characterized by a micro-corrugation in the channel wall perpendicular to the exhaust gas flow. This corrugation supports the development of a radial flow component in the boundary layer, thus enhancing the mass transfer between the exhaust gas and the wall. The improved mass transfer of a TS substrate can be translated into either a more efficient or smaller catalyst [1,2].

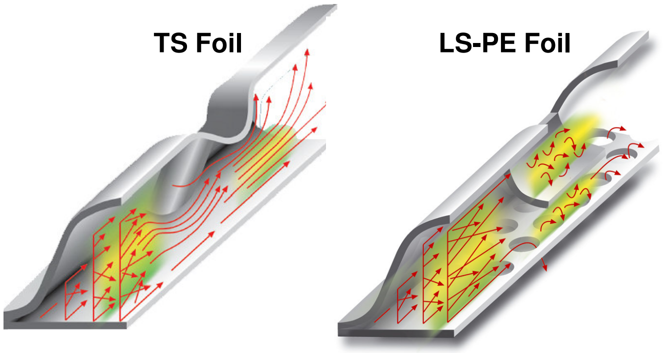

Figure 1. Schematic illustration of the TS and LS-PE metallic foils showing introduction of turbulence by secondary structures. The LS foil is the same as LS-PE foil except with a solid (unperforated) base.

LONGITUDINAL FOIL STRUCTURE (LS, LS-PE)

The LS foil is characterized by shovels protruding into the flow channel which transform laminar channel flow into turbulent flow. This creates enhanced mass transfer between the exhaust gas and substrate walls. This effect is illustrated for both TS and LS foils in Figure 2. Over the length of a channel, the flow disturbances of the LS and TS foils provide more mass transfer than a standard straight channel foil. The effect is especially pronounced in the case of the LS foil.

As shown in Figure 1, LS-PE is an alternating combination of a LS foil and a perforated foil (PE) which allows exhaust cross flow within the substrate. In addition, perforating the foils reduces the substrate's thermal mass, which can improve its light-off characteristic [6].

Figure 2 shows an example of calculated mass transfer for various types of 200 cpsi substrates at specified conditions. The mass transfer coefficient, Beta, shown in Figure 2 was calculated with the following relationship.

$$\beta = \frac{Sh\, D_{12}}{d_{hydr.}} \qquad [5]$$

In the equation above, *Sh* is the Sherwood number, D_{12} is the Diffusion coefficient and $d_{hydr.}$ is the hydraulic diameter of the substrate channel.

As shown in the figure, the LS foil produced two substantial mass transfer peaks that are generated by gas entering and exiting each of the shovel structures.

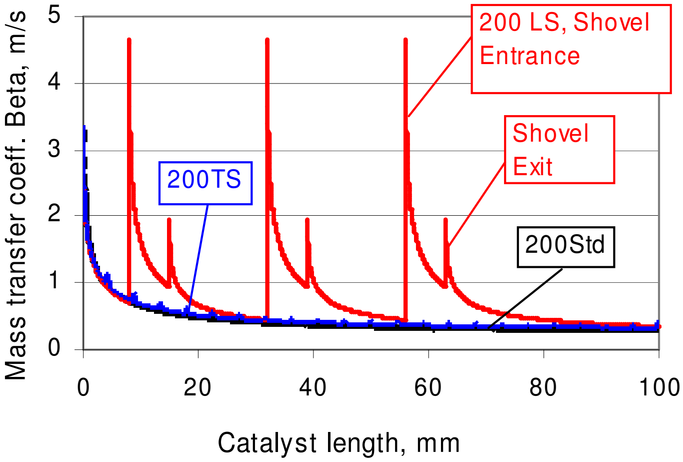

Figure 2. Calculated mass transfer coefficients of TS and LS foils compared to a standard straight channel substrate as a function of catalyst length. (Temperature = 700°C, Channel Velocity = 50m/s).

In addition, the interrupted channel walls of the LS substrate allow cross flow of the exhaust gas from one channel to neighboring channels. If uneven flow distribution is present in front of the catalyst, this flow exchange can improve surface area utilization [3,6]. Both effects, enhanced mass transfer and better surface area utilization, can provide equivalent performance to continuous channel substrates at a lower cell density or smaller volume.

EXPERIMENTAL DESIGN

This experiment was designed to determine if an advanced metallic substrate with less precious metal loading could adequately replace a baseline ceramic substrate in a diesel oxidation catalyst environment.

SUBSTRATES

The following testing was designed to compare a baseline ceramic DOC with three different metallic DOCs in the same experimental environment. As discussed below, the ceramic baseline DOC was sized to exactly replace the total volume of the three DOCs found on the production vehicle. In order to understand if the theoretical benefit of better mass transfer of the advanced metallic substrates could be translated into better DOC performance, the size of the three metallic substrates was reduced by up to 30% of the baseline ceramic DOC volume.

Each substrate was carefully coated with 3.2 g/L (90 g/ft^3) of a Pd stabilized Pt diesel oxidation catalyst. Therefore, the smaller metallic substrates were coated with less precious metal than the larger ceramic substrate. In addition, the amount of base washcoat was adjusted to achieve a nearly constant washcoat thickness over the substrate surface area.

The configuration, dimensions, and platinum group metal (PGM) loading for all tested substrates are shown in Table 1.

Table 1. Substrate configuration, dimensions, and precious metal loadings.

Substrate (CPSI/WT)*	**D (mm)**	**Length (mm)**	**Volume (L)**	**GSA† (m^2)**	**PGM (g)**
Ceramic (400/6.5)	152.4	208 (2x104)	3.8 (2x1.9)	10.5	12 (6x2)
Metallic TS (400/0.04)	150	160	2.8	9.5	9
Metallic LS (300/0.04)	150	150	2.7	7.8	8.5
Metallic LSPE (300/0.04)	150	140	2.5	6.2	7.9

** CPSI, Cells per square inch; WT, Wall thickness, mm*
† GSA = Geometric Surface Area

VEHICLE MODIFICATIONS

A production European sedan with a 2.7L twin turbocharged diesel V-6 was chosen for this evaluation. This vehicle came standard with three DOCs. A DOC was close coupled to each turbo and a third DOC was installed directly in front of a diesel particulate filter (DPF). The combined volume of all three production DOCs was 3.8L.

These three DOCs were removed and replaced with a single underbody DOC. Each catalyst was packaged identically with the same sensor locations to minimize experimental variability. The test assembly is shown schematically in Figure 3.

The production exhaust system was not insulated from the environment. To conserve heat and compensate for moving a substantial portion of the production DOC volume downstream, the entire exhaust (from the turbocharger outlet to the rear of the DPF) system was insulated with several layers of insulating wrap. A picture of the production and modified exhaust systems is shown in Figure 4.

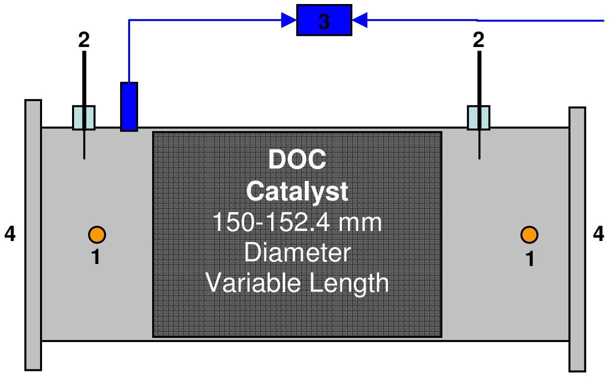

Tag	Name
1	Sample ports
2	Thermocouples (1.6mm Diameter)
3	Differential pressure sensor
4	Marmon flanges (Low thermal mass)

Figure 3. Standard DOC can line drawing with sensor locations.

DYNAMOMETER TESTING

All testing was preformed at Ford's Vehicle Emissions Research Laboratory (VERL-1) chassis dynamometer facility. VERL-1 contains a full suite of real-time emissions measurement equipment, including four emissions analysis systems (Each system independently measures HC, CO, NO_x and CO_2), a Fourier transform Infrared (FTIR) spectrometer, and mass spectrometer for emissions speciation.

Before testing, each DOC was degreened using a standard oven aging cycle. The degreened DOCs were loaded in the exhaust and allowed to soak overnight or until the engine and exhaust temperatures equilibrated to room temperature.

Each DOC was tested over several FTP-72 and US-06 test cycle separated by a 180s idle period. This unique combination of cycles was selected to economize testing time while illuminating the most important facets of DOC operation. The FTP-72 consists of the first two bags of the more common FTP-75 test cycle. It was chosen to understand the effect of cold start and light loads on the DOC substrates. The US-06 cycle was chosen to understand the effect of high loads and transients.

DOC substrates were tested in random order and repeated in a different order until the variance in the tailpipe hydrocarbon emissions were within a 5% margin. For this data, three to five tests were run on each substrate and averaged for the final data. All data was collected at a minimum frequency of 1Hz.

Before Modification

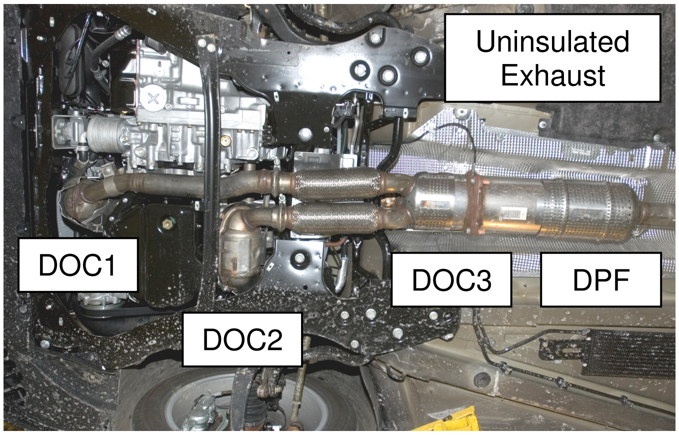

After Modification

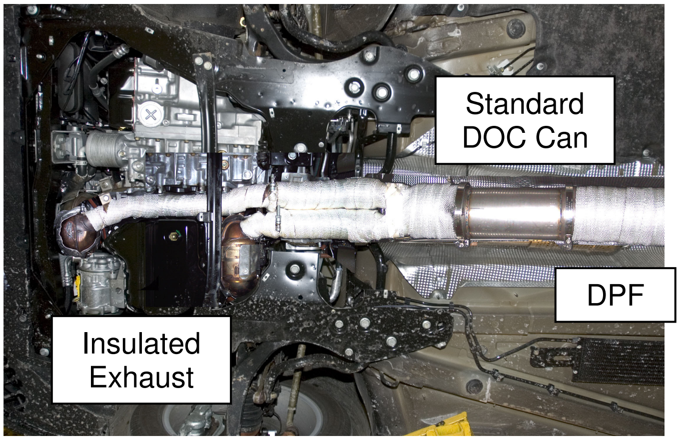

Figure 4. Photographs of the diesel exhaust system before and after modification. In the after modification photo, the standard DOC can is shown uninsulated for clarity.

RESULTS & DISCUSSION

The accumulated tailpipe hydrocarbon performance of the four DOCs over the FTP-72/US-06 test cycle described above is compared in Figure 5. The TS and LSPE metallic DOCs performed on par with the ceramic DOC. The LS metallic outperformed all DOCs by a significant margin, emitting 25% less hydrocarbons than its ceramic counterpart. This difference is almost entirely attributed to the first 60 seconds of operation from cold start.

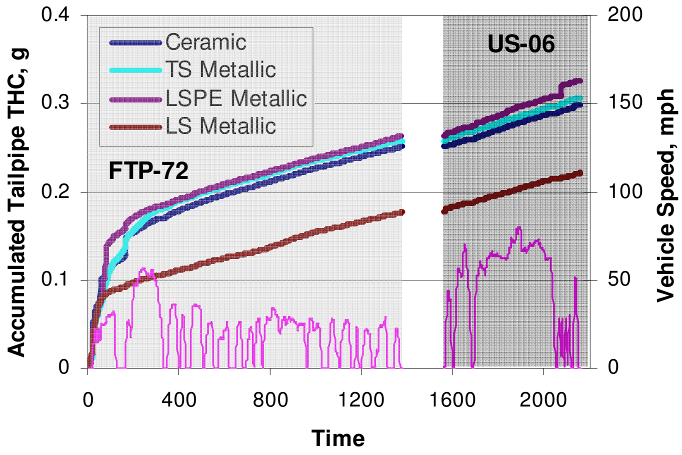

Figure 5. Accumulated tailpipe hydrocarbons over the FTP-72 and US-06 test cycles.

The DOC exit temperature and instantaneous tailpipe hydrocarbons for each DOC during the first 100 seconds of the FTP-72 are shown in Figure 6 and 7 respectively. Unfortunately, LSPE temperature data was not available due to an error in the data acquisition system. In the first minute of cold start, the smaller LS DOC heated faster and maintained higher temperatures than the larger TS or ceramic DOCs

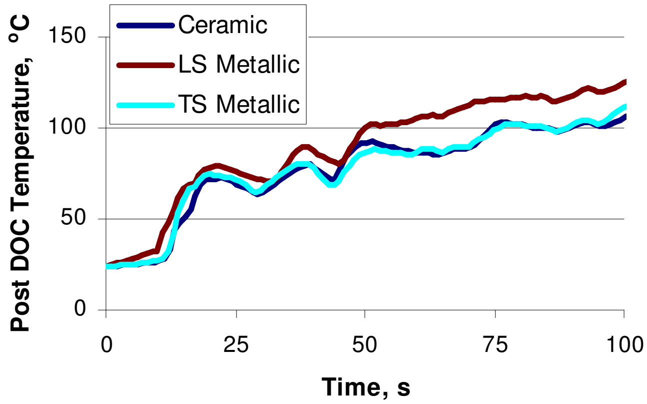

Figure 6. Exhaust gas temperatures at the exit of the DOC over the FTP-72 and US-06 test cycles.

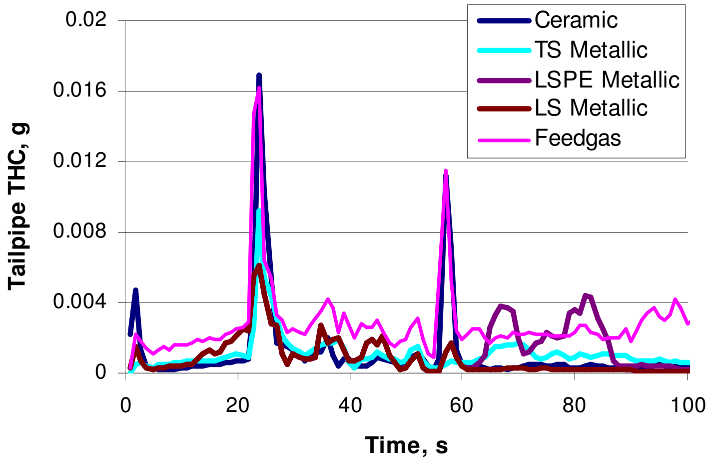

Figure 7. Tailpipe hydrocarbons over the FTP-72 and US-06 test cycles.

During cold-start, the faster heat-up of the LS substrate coupled with the enhanced mass transfer and turbulence generated by its longitudinal shovels reduced the amount of time necessary for the substrate to reach light-off temperature.

When this data is compared to the tailpipe hydrocarbon data in Figure 5, it is evident that the low thermal mass of the LS substrate coupled with the enhanced mass transfer of its longitudinal shovels provides a unique advantage over continuous channel substrates (TS and ceramic) in a DOC environment.

However, the LS-PE DOC did not lightoff as well as the LS substrate. It is thought that the reduced surface area of the perforated foil coupled with the reduced amount of washcoat and hydrocarbon storage capacity is the cause of this difference. It is possible that improvements in washocat technology could reverse this trend.

The pressure drop of each DOC was measured with the DPF over the FTP-72/US-06 test cycle described above. Unfortunately, the different DPF soot loading in each DOC test confounded a direct comparison of DOC pressure drop.

Instead, the pressure drop of each of the substrates was calculated with the traditional theoretical approach to describe laminar flow in tubes and was extended with terms to account for interruptions in the channel wall (PE) or reduced in the region of the shovel (LS) [4]. To represent flow characteristics at the shovel inlet (LS) and the end of a hole (PE), turbulent contributions were added to the model. As shown in Figure 8, the pressure drop of the metallic DOCs is always less than the ceramic DOC due to their thinner walls, shorter length, and/or lower cell densities. For the 2.7L engine at its 630 kg/hr maximum exhaust flow, all the metallic substrates showed lower pressure drop than the ceramic baseline (0.17 mm wall thickness).

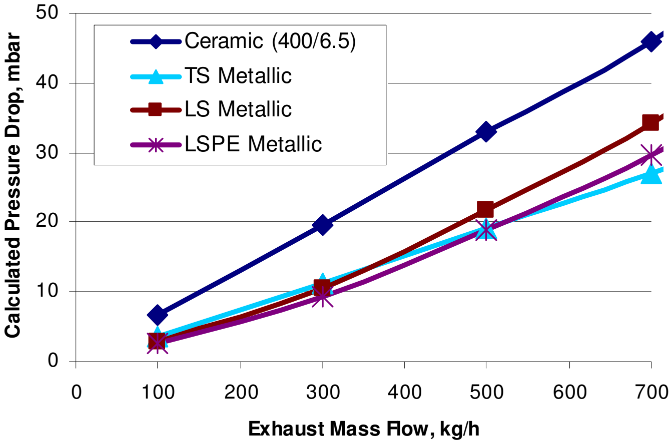

Figure 8. Calculated pressure drop over 700 kg/hr mass flow for part sizes shown in Table I assuming 1.2 bar absolute pressure after the DOC and 350°C.

CONCLUSIONS

A collection of three advanced metallic and one ceramic DOC were tested on a production 2.7L diesel vehicle. To understand the opportunity of the advanced metallic structures, all metallic substrates were sized to equivalent DOC performance and coated with up to 30% less precious metal than the ceramic oxidation catalyst.

The results over FTP-72 and US-06 test cycles showed the advanced metallic DOCs preformed on par or better than the ceramic DOC in terms of hydrocarbon conversion, heat-up, and pressure drop. The differences observed in conversion and heat-up were attributed to the higher thermal conductivity and lower thermal mass of the metallic as well as the increased mass transfer, mixing, and turbulence resulting from their secondary shovel structures.

The difference in pressure drop was attributed simply to the thinner walls, shorter lengths, and lower cell densities of the metallic structures.

REFERENCES

1. SAE 940932 “Improved Cell Design for Increased Catalytic Conversion Efficiency," W. Held, M.Rohlfs, VW AG, W.Maus, H. Swars, R. Brueck, F. Kaiser, Emitec GmbH
2. SAE 950788 “Flow Improved Efficiency by New Cell Structures in Metallic Substrates," R.Brueck, J. Diringer, U. Martin, W. Maus, Emitec GmbH
3. SAE 2004-01-1488 “Next Generation Catalysts are turbulent – Development of Support and Coating," M. Bollig, J. Liebel, R. Zimmer, BMW Group, M. Kraum, O.Seel, S. Siegmung, Engelhard Technologies GmbH, R. Brueck, J. Diringer, W. Maus, Emitec GmbH
4. VDI-Wärmeatlas; Bohl, Technische Strömungslehre, Vogel-Verlag
5. S. Kakac & Y. Yener, "Convective Heat Transfer," Second Edition, CRC Press, 1994
6. SAE 2005-01-3851 "Innovative Metallic Substrates for Exhaust Emission Challenges for Gasoline and Diesel Engines," K Mueller-Haas, M. Rice